ELSEVIER

Journal of Alloys and Compounds 434–435 (2007) 594–597

Journal of ALLOYS AND COMPOUNDS

www.elsevier.com/locate/jallcom

Magnetic and magnetotransport properties in metastable granular systems

P. Tiberto [a,*], P. Allia [b], M. Baricco [c], M. Coïsson [a], F. Vinai [a]

[a] *IEN Galileo Ferraris, Strada delle Cacce 91, I-10135 Torino, Italy*
[b] *Politecnico di Torino, Dipartimento di Fisica, I-10129 Torino, Italy*
[c] *Dipartimento di Chimica IFM and NIS, Università di Torino, Via P. Giuria 9, 10125 Torino, Italy*

Available online 11 October 2006

Abstract

A negative, isotropic magnetoresistance (MR) has been measured in a wide class of nanogranular magnetic materials produced by off-equilibrium techniques. The common feature of these magnetic systems is the granularity, either structural or magnetic, on the nanometer scale. In this work analogies and differences among magnetotransport effects observed in bi-metallic alloys, either in bulk or thin-film form, will be highlighted. In addition, the role and nature of interparticle interaction on magnetic and magnetotransport properties of nanogranular systems will be discussed.

Keywords: Magnetic films; Rapid solidification; Quenching; Magnetoresistance; Magnetic measurements

1. Introduction

The giant magnetoresistance (MR) of bi-metallic granular systems has been related to the reorientation of magnetic moments, and is interpreted on the basis of spin-dependent scattering of conduction electrons [1,2]. In the last decade, different measurements have revealed that a negative isotropic magnetoresistance is a common feature of a wide class of nanostructured magnetic materials. Very similar effects have emerged in various magnetic systems, both diluted and concentrated, such as Curie–Weiss paramagnets, core–shell nanoparticulate materials, bulk frustrated ferromagnets, whose common feature is the loss of magnetic coherence on the nanometer scale. In particular, a negative magnetoresistance has been observed in the bulk alloy $Au_{80}Fe_{20}$, both above and below the paramagnetic Curie temperature, and in chemically homogeneous, frustrated ferromagnets such as $Au_{70}Fe_{30}$ and $Cu_{60}Fe_{20}Ni_{20}$ [3–5]. This effect has been called proximity magnetoresistance (PMR) since, contrary to the case of superparamagnetic particles of conventional bimetallic granular systems, the primary magnetic scatterers are identified as the edges of adjacent regions of magnetic coherence having size comparable to the electronic mean free path. Basically, all MR effects have the same microscopic origin at an atomic level; the magnetoresistive response of all the above mentioned magnetic systems may be exploited to get information about the extent of magnetic correlation on the scale of the electronic mean-free path.

Two bimetallic alloy families exhibiting notable magnetoresistance effects are $Cu_{100-x}Co_x$ and $Au_{100-x}Fe_x$. Different from the case of $Cu_{100-x}Co_x$ systems, $Au_{100-x}Fe_x$ alloys are not easily obtained in granular form by rapid solidification: quenching from either liquid or solid phases produces a homogeneous disordered alloy, characterised by a cluster-glass behaviour below a transition temperature which is below room temperature for $x = 20$ at.% [3]. Co-sputtering has been effectively exploited to produce nanogranular $Au_{100-x}Fe_x$ systems [6]. This work is focused on both $Cu_{100-x}Co_x$ and $Au_{100-x}Fe_x$ produced by means of different off-equilibrium techniques either as nanogranular systems or as chemically homogeneous alloys. An overview of their magnetoresistance properties will be given, highlighting common aspects and peculiarities among bulk alloys and thin films of the same nominal composition. In addition, the role and nature of interparticle interaction on magnetic and magnetotransport properties of nanogranular systems will be discussed.

2. Experimental

A continuous ribbon of nominal composition $Cu_{95}Co_5$ has been produced by rapid solidification in an inert atmosphere by planar flow casting on a rotating Cu–Zr drum. Continuous ribbons of $Au_{100-x}Fe_x$ ($x = 20$ and 30 at.%) have been casted by rapid solidification from the melt by means of the standard melt-spinning technique in vacuum (width 2 mm, average thickness 120 mm). $Au_{100-x}Fe_x$ ($x = 20$ and 30 at.%) films of thickness 1.5 mm have been grown on

* Corresponding author. Tel.: +39 011 3919857; fax: + 39 011 3919834.
E-mail address: tiberto@inrim.it (P. Tiberto).

0925-8388/$ – see front matter © 2006 Elsevier B.V. All rights reserved.
doi:10.1016/j.jallcom.2006.08.088

a Si (1 0) substrate by dc magnetron co-sputtering in Ar. An extraction magnetometer (temperature range: 2–350 K; magnetic field range: 0–70 kOe) and a vibrating sample magnetometer (temperature range: 300–700 K; magnetic field range: 0–20 kOe) have been exploited for magnetic measurements. Magnetoresistance measurements have been performed between 4 and 300 K by means of the four-contact method with soldered electrical contacts, under the in-plane applied field provided by the MagLab system (maximum value: 70 kOe). The magnetoresistance response MR is defined as $[R(H) - R(0)]/R(0) \times 100$.

3. Results and discussion

Magnetisation curves of the as-cast $Cu_{95}Co_5$ ribbon are reported in Fig. 1a as a function of temperature. Typical superparamagnetic features with unsaturating behaviour at high fields are observed at all temperatures. As expected, the high field magnetisation M_s increases with decreasing temperature. By considering that the ideal saturation value of this alloy would be ≈74 emu/g, the attained M_s value measured at $T = 5$ K indicates that only ≈50% of Co has segregated during the rapid solidification process, the remaining fraction being still dissolved in the metallic matrix. The field behaviour of the magnetoresistance measured at the same temperatures is reported in Fig. 1b. Again, no saturation is observed at all studied temperatures. As expected, the MR ratio is seen to increase with decreasing T, reaching values as high as 9%. This effect can be better described by plotting the MR as a function of reduced magnetization m (see Fig. 1c). For a random distribution of non-interacting magnetic scatterers, the magnetoresistance ratio should be a quadratic function of the reduced magnetization $m = M(H)/M_s$. Deviation of the MR(m) curve from the parabolic behavior has been ascribed either to a distribution of particle size or, with some plausibility and experimental support, to magnetic correlation among scatterers [7,8]. In the present case, an almost parabolic behavior is observed at $T = 270$ K; this indicates that Co particles precipitated during the rapid solidification process are statistically independent. At lower temperatures a flat-top parabola is observed, pointing to the fact that the magnetic correlation among magnetic moments is no longer negligible [8]. The room-temperature magnetisation curves of $Au_{80}Fe_{20}$ bulk alloy and thin film are reported in Fig. 2 together with $Au_{70}Fe_{30}$ bulk alloy. No significant hysteresis is observed in all samples. A paramagnetic behavior is observed for the $Au_{80}Fe_{20}$ bulk alloy, whose Curie temperature is ≈290 K [3]. On the contrary, the

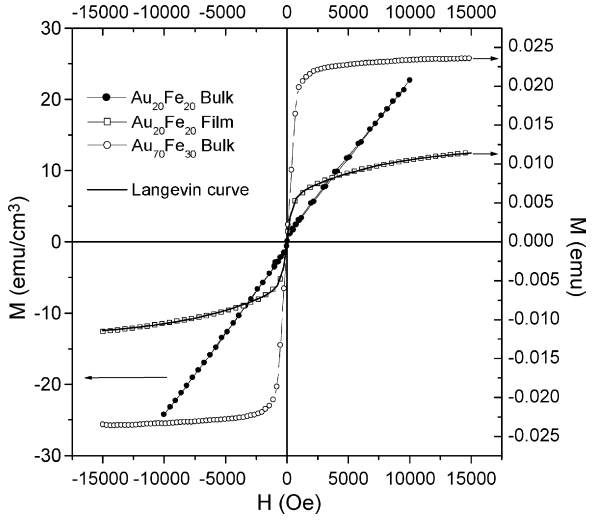

Fig. 2. Magnetisation curves measured at $T = 300$ K of $Au_{80}Fe_{20}$ bulk alloy and thin film together with $Au_{70}Fe_{30}$ bulk alloy.

magnetisation curve of co-sputtered $Au_{80}Fe_{20}$ displays a superparamagnetic behavior, as confirmed by the excellent fit with a single Langevin curve (continuous line in Fig. 2). A completely different magnetic regime typical of frustrated ferromagnets is observed in the $Au_{70}Fe_{30}$ bulk alloy: here, a first magnetization jump at low-fields is followed by a slow approach to saturation. The room-temperature magnetoresistance curves are reported in Fig. 3a as functions of magnetisation for $Au_{100-x}Fe_x$ bulk alloys ($x = 20$ at.%) and of m ($x = 30$ at.%). A nearly perfect parabolic behavior is observed for the paramagnetic bulk alloy $Au_{80}Fe_{20}$, clearly indicating that the magnetic moments of the scattering units (in this case a single Fe atom or clusters formed by a few tens of atoms) are statistically uncorrelated, precisely as expected for a paramagnetic system. On the contrary, the MR of $Au_{70}Fe_{30}$ bulk alloy is almost zero in correspondence of the low-field magnetisation jump, becoming rather strong in correspondence of the slow approach to saturation at high field. This experimental behavior is connected with the two-step magnetisation behavior typical of frustrated ferromagnets, where the low field magnetisation jump is related to coherent rotations of regions having linear dimensions definitely larger than electronic mean free path λ. With increasing H, the magnetization process involves further alignment of spins located at distances

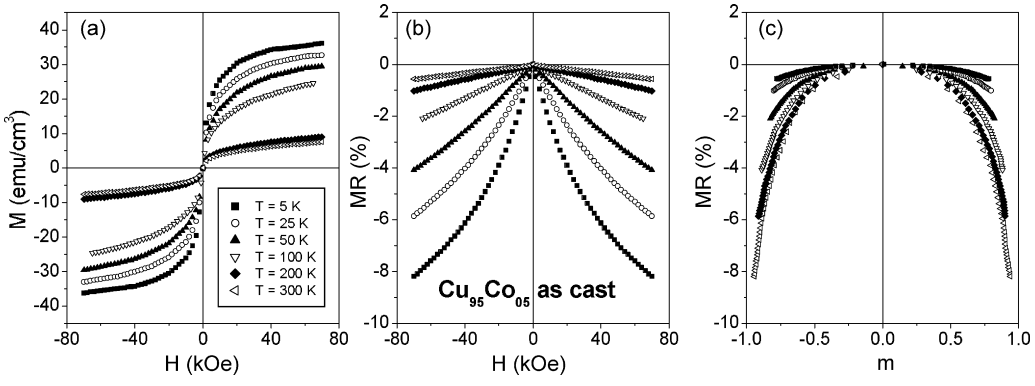

Fig. 1. (a) Magnetisation curves, (b) MR vs. H behavior and (c) MR ratio as a function of m measured at selected temperatures for as-cast $Cu_{95}Co_5$ ribbon.

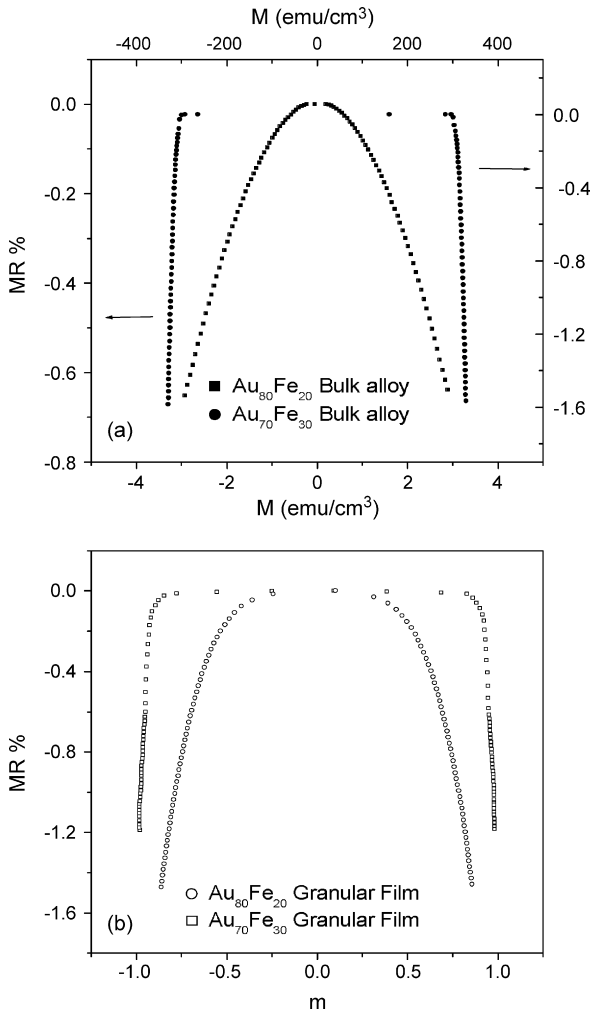

Fig. 3. (a) Room-temperature behavior of MR vs. m in $Au_{100-x}Fe_x$ bulk alloys (b) same as in (a) for thin films.

of the order of λ, giving rise to the observed MR. This box-like shape of MR versus m curve is the distinctive feature of the PMR effect occurring in *magnetically* inhomogeneous systems such as these frustrated ferromagnets, where the magnetic scatterers are the edges of adjacent magnetic regions whose magnetisation is blocked by competing interactions. The room-temperature MR versus m curves of $Au_{80}Fe_{20}$ and $Au_{70}Fe_{30}$ thin films are reported in Fig. 3b. A flat-top parabola is observed for the granular $Au_{80}Fe_{20}$ system, while a box-like behavior is observed for the sample with $x = 30$ at.%. The co-sputtered film $Au_{80}Fe_{20}$ is therefore found to have magnetic properties different from those of the bulk alloy of the same composition, i.e., closer to those of a granular system with interacting nanoparticles. Macroscopically homogeneous solid solutions of $Au_{100-x}Fe_x$ are known to exhibit complex metallurgical features (i.e. composition fluctuations, Guinier–Preston zones) that are presumably the origin of their magnetic and magnetoresistive properties; however, all weak compositional fluctuations disappear in samples produced by co-sputtering, intrinsically providing strong compositional inhomogeneities.

We have just seen how markedly different can be the shape of the MR versus m curves in dependence of an alloy's composition and preparation. According to a recent theory, it is possible to quantitatively relate the MR versus m curve to the range of magnetic correlation among scatterers and to its changes with both field and temperature [9]. In this way, the nanoscale magnetic properties of frustrated metallic ferromagnets can be inferred. At fixed T, it is expected that the correlation among two magnetic moments is lost at high fields. In the frame of this phenomenological model, a magnetic correlation range R_m is obtained using the following expression [9]:

$$R^* - R = \alpha[(\langle u^2\rangle - \langle u\rangle^2)e^{-\lambda/R_m} + (1 - \langle u^2\rangle)e^{-2\lambda/R_m}] \quad (1)$$

where R is the measured electrical resistance, R^* the parabolic resistance deriving from high-field resistance fit, α a constant, $\langle u\rangle$ the thermal average of the cosine of the angle between magnetic moments and the field axis (it is therefore coincident with the reduced magnetization m), and $\langle u^2\rangle = 1/3 + 2/3\langle u\rangle^3$ according to a random-walk model [9]; the value of the electronic mean free path λ is extracted from zero-field resistance measurements.

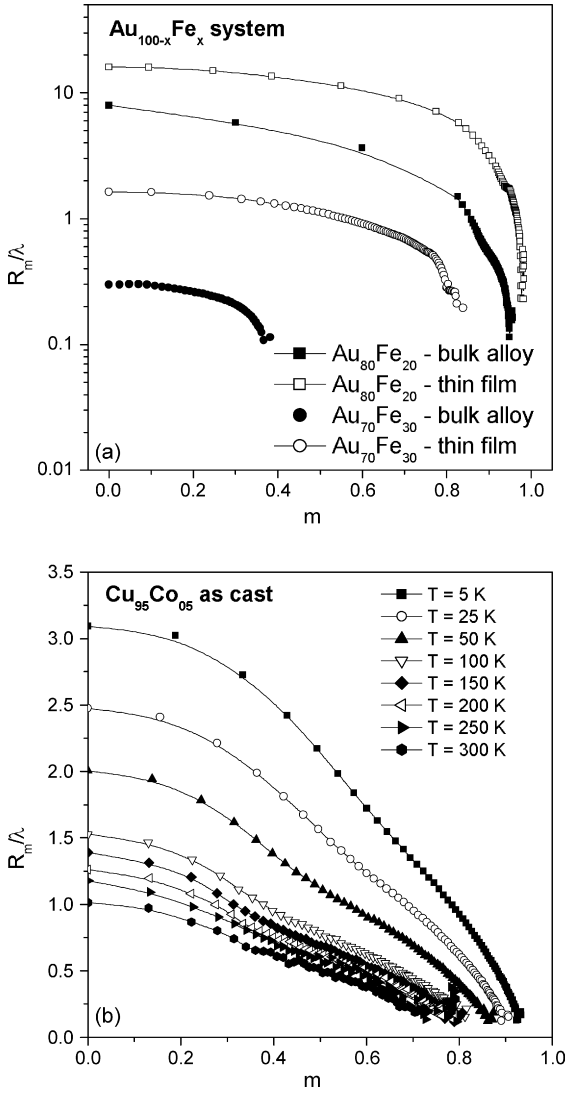

Fig. 4. (a) R_m/λ vs. m behavior at room-temperature for $Au_{100-x}Fe_x$ bulk alloys and thin films; (b) R_m/λ vs. m behavior at selected temperature for as cast $Cu_{95}Co_5$.

The quantity R_m represents the average radius of magnetic correlation between magnetic scatterers [9]. Actually, Eq. (1) holds in bulk frustrated magnets; in principle, in granular systems this equation should be substituted by a formula including two distinct correlation ranges for the Euler angles θ and ϕ; however, Eq. (1) can be exploited even in this case, because of the linear correlation experimentally observed between R_θ and R_ϕ [8]. According to this simple theory, any deviation from the parabolic behavior is attributed to correlation among moments rather than to other causes such as particle size distribution [7]. Eq. (1) allows one to univocally determine the correlation ratio R_m/λ for each material, and its dependence on both temperature and magnetic field (or magnetisation). The room-temperature R_m/λ behavior is reported in Fig. 4a as a function of m for $Au_{100-x}Fe_x$ bulk alloys. Substantially lower values of R_m/λ are observed in the alloy with lower Fe content. In the $Au_{80}Fe_{20}$ bulk alloy R_m/λ is lower than unity, confirming the simple picture of statistically independent magnetic moments. On the contrary, in both the $Au_{70}Fe_{30}$ systems the magnetic moments are correlated over nanometer-size lengths. The behaviour of R_m/λ is reported in Fig. 4b for the $Cu_{95}Co_{05}$ granular ribbon at selected temperatures. This ratio monotonically decreases with increasing m at any temperature, as predicted [9]. In a granular system, the starting value $R_m(H=0)/\lambda$ versus m decreases with temperature because the equilibrium size of correlated regions is increasingly reduced [9].

In conclusion, the magnetoresistance turns out to be a property very sensitive to the nanoscale structure of metastable bimetallic magnetic systems, as determined by composition and preparation procedure. In particular, the combination of MR measurements with magnetic properties has been shown to be a very powerful tool to obtain information on the nanometric magnetic coherence region. Moreover, the magnetoresistance analysis allows one to gain insight on magnetic structures extending on the nanometer length scale, that are hardly observable by other experimental means.

Acknowledgment

This work has been supported by FIRB-MIUR/INFM project RBNE017XSW.

References

[1] S. Zhang, P.M. Levy, J. Appl. Phys. 73 (1993) 5315.
[2] J.Q. Xiao, J.S. Jiang, C.L. Chien, Phys. Rev. Lett. 68 (1992) 3749.
[3] P. Allia, M. Coisson, J. Moya, V. Selvaggini, P. Tiberto, F. Vinai, Phys. Status Solidi 189 (2002) 321.
[4] P. Allia, M. Coisson, V. Selvaggini, P. Tiberto, F. Vinai, Phys. Rev. B63 (2002) 180404R.
[5] P. Allia, M. Coisson, J. Moya, V. Selvaggini, P. Tiberto, F. Vinai, E. Bosco, Mater. Sci. Eng. A 375–377 (2004) 1006.
[6] P. Allia, F. Celegato, M. Coisson, A. Da Re, F. Ronconi, F. Spizzo, P. Tiberto, F. Vinai, J. Magn. Magn. Mater. 190–291 (2005) 280.
[7] E.F. Ferrari, F.C.S. da Silva, M. Knobel, Phys. Rev. B56 (1997) 6086.
[8] P. Allia, M. Knobel, P. Tiberto, F. Vinai, Phys. Rev. B52 (1995) 15398.
[9] P. Allia, M. Coisson, J. Moya, V. Selvaggini, P. Tiberto, F. Vinai, Phys. Rev. B67 (2003) 174412.